

IR Spectroscopy of $\text{Nb}^+(\text{N}_2)_n$ Complexes: Coordination, Structures, and Spin States

E. Dinesh Pillai, Todd D. Jaeger, and Michael A. Duncan*

Contribution from the Department of Chemistry, University of Georgia, Athens, Georgia 30602

Received August 22, 2006; E-mail: maduncan@uga.edu

Abstract: Infrared photodissociation spectroscopy in the N–N stretching region is reported for gas-phase $\text{Nb}^+(\text{N}_2)_n$ complexes ($n = 3–16$). The coordination of nitrogen to the metal cation causes the IR-forbidden N–N stretch of N_2 to become active in these complexes. Fragmentation occurs by the loss of intact N_2 molecules, and the yield as a function of laser wavelength produces an IR excitation spectrum. The dissociation patterns indicate that Nb^+ has a coordination of six ligands. The infrared spectra for all complexes contain bands red-shifted from the N–N stretch in free nitrogen, consistent with ligand–metal charge-transfer interactions such as those familiar for metal carbonyl complexes. Using density functional theory, we investigated the structures and ground electronic states for each of the small cluster sizes. Theory indicates that binding to the low-spin triplet excited state of the metal ion becomes progressively more favorable than binding to its high-spin quintet ground state as additional ligands are added to the cluster. Although the quintet state is the ground state for the $n = 1–4$ complexes, IR spectroscopy confirms that the low-spin triplet electronic state becomes the ground state for the $n = 5$ and 6 complexes. The $n = 4$ complex has a square-planar structure, familiar for high-spin d^4 complexes in the condensed phase. The $n = 5$ complex has a geometry that is nearly a square pyramid, while the $n = 6$ complex has a structure close to octahedral.

Introduction

Biological and catalytic systems contain numerous examples of molecular nitrogen interacting with transition metals (TM).^{1–8} The natural catalyst for nitrogen fixation is an enzyme that carries Fe, Mo, and V at its active sites.^{1–5} TM–nitrogen interactions are also important in the synthesis of ammonia.^{6–8} The dissociation of N_2 by catalytic iron surfaces is the rate-determining step in this process, although the mechanism is not yet fully understood.^{7,8} Model studies of gas-phase metal clusters may provide insight into the chemistry of these systems.^{2,3} TM–nitrogen complexes are isoelectronic to TM–carbonyl complexes, which are prototypical systems in coordination chemistry, inorganic chemistry, and organometallic chemistry.^{9–12} Hence, there has been a longstanding theoretical and experi-

mental interest in metal containing nitrogen compounds to draw comparisons between N_2 and CO as ligands.¹³ In this article, we investigate the bonding interactions between Nb^+ and N_2 ligands by probing the N–N vibration in $\text{Nb}^+(\text{N}_2)_n$ complexes with infrared photodissociation spectroscopy (IRPD).

There has been substantial interest in model TM–nitrogen complexes, and these systems have been studied by theory,^{14–16} mass spectrometry,^{17,18} and spectroscopy.^{19–23} Initial theoretical efforts have focused on the Fe– N_2 complex due to its relevance in biochemistry and catalysis, and its structures and bonding energetics have been investigated.^{14–16} Collision-induced dissociation has been used to measure bond energies for various first-row TM⁺–nitrogen complexes,¹⁷ whereas various spectroscopy methods have probed their structures.^{19–22} Second-

- (1) Seigbahn, P. E. M.; Blomberg, M. R. A. *Chem. Rev.* **2000**, *100*, 421.
- (2) Burgess, B. K.; Lowe, D. K. *Chem. Rev.* **1996**, *96*, 2983.
- (3) Rincon, L.; Ruetter, F.; Hernandez, A. *J. Mol. Spectrosc.* **1992**, *254*, 395.
- (4) (a) Fryzuk, M. D. *Chem. Rev.* **2003**, *3*, 2. (b) Fryzuk, M. D.; Kozak, C. M.; Patrick, B. O. *Inorg. Chim. Acta* **2003**, *345*, 53.
- (5) (a) Chatt, J.; Melville, D. P.; Richards, R. L. *J. Chem. Soc. A* **1969**, *18*, 2841. (b) Chatt, J.; Dilworth, J. R.; Richards, R. L. *Chem. Rev.* **1978**, *78*, 589. (c) Richards, R. L. *Coord. Chem. Rev.* **1996**, *153*, 83.
- (6) Somorjai, G. A. *Introduction to Surface Chemistry and Catalysis*; Wiley: New York, 1994.
- (7) Rao, C. N. R.; Rao, G. R. *Surf. Sci. Rep.* **1991**, *13*, 221.
- (8) Arabczyk, W.; Jasinska, I.; Lubkowski, K. *React. Kinet. Catal. Lett.* **2004**, *83*, 385.
- (9) (a) Cotton, F. A.; Wilkinson, G.; Murillo, C. A.; Bochmann, M. *Advanced Inorganic Chemistry*, 6th ed.; Wiley: New York, 1999. (b) Huheey, J. E.; Keiter, E. A.; Keiter, R. L. *Inorganic Chemistry: Principles of Structure and Reactivity*, 4th ed.; HarperCollins: New York, 1993.
- (10) Zhou, M.; Andrews, L.; Bauschlicher, C. W., Jr. *Chem. Rev.* **2001**, *101*, 1931.
- (11) Ervin, K. M. *Int. Rev. Phys. Chem.* **2001**, *20*, 127.
- (12) Frenking, G.; Frohlich, N. *Chem. Rev.* **2000**, *100*, 717.
- (13) (a) Chatt, J. *Pure Appl. Chem.* **1970**, *24*, 425. (b) Chatt, J. *J. Organomet. Chem.* **1975**, *100*, 17. (c) Chatt, J.; Richards, R. L. *J. Organomet. Chem.* **1982**, *239*, 65.
- (14) Bauschlicher, C. W., Jr.; Petterson, L. M.; Siegbahn, P. E. M. *J. Chem. Phys.* **1987**, *87*, 2129.
- (15) Zacarias, A.; Torrens, H.; Castro, M. *Int. J. Quantum Chem.* **1997**, *61*, 467.
- (16) Duarte, A. D.; Salahub, D. R.; Haslett, T.; Moskovits, M. *Inorg. Chem.* **1999**, *38*, 3895.
- (17) (a) Khan, F. A.; Steele, D. L.; Armentrout, P. B. *J. Phys. Chem.* **1995**, *99*, 7819. (b) Tjelta, B. L.; Armentrout, P. B. *J. Phys. Chem.* **1997**, *101*, 2064. (c) Tjelta, B. L.; Walter, D.; Armentrout, P. B. *Int. J. Mass Spectrom.* **2001**, *204*, 7.
- (18) Heinemann, C.; Schwarz, J.; Schwarz, H. *J. Phys. Chem.* **1996**, *100*, 6088.
- (19) Lever, A. B. P.; Ozin, G. A. *Inorg. Chem.* **1997**, *16*, 2012.
- (20) Asher, R. L.; Buthelezi, B.; Brucat, P. J. *J. Phys. Chem.* **1995**, *99*, 1068.
- (21) (a) Andrews, L.; Bare, W. D.; Chertihin, G. V. *J. Phys. Chem. A* **1997**, *101*, 8417. (b) Zhou, M.; Andrews, L. *J. Phys. Chem. A* **1998**, *102*, 9061.
- (22) Green, D. W.; Hodges, R. V.; Gruen, D. M. *Inorg. Chem.* **1976**, *15*, 970.
- (23) Parrish, S. H.; Van Zee, R. J.; Weltner, W., Jr. *J. Phys. Chem. A* **1999**, *103*, 1025.

row TM–ligand chemistry is appealing because these metals are usually more reactive than their first-row counterparts and hence can trigger ligand activation and dissociation.^{9,12,24,25} Consequently, the reactivity of second-row TMs toward various ligands has been examined by theoretical methods²⁶ and gas-phase kinetics measurements.^{27,28} Motivated by this, researchers have undertaken a number of studies to investigate the reactivity of neutral and ionic Nb complexes and multimetal Nb atom clusters.^{29–35} Armentrout and co-workers have studied the activation of small hydrocarbons by Nb⁺.²⁹ Matrix isolation infrared spectroscopy has been applied to neutral Nb(N₂)_n complexes to determine their structures.^{21,22} Electron-spin resonance spectroscopy coupled with matrix isolation has been applied to neutral Nb(N₂)₆ and Nb(CO)₆ complexes.²³ Various groups have studied the size-specific reactivity of neutral and ionic Nb clusters with small molecules such as N₂,^{30–32} CO,³¹ D₂,³² NO, and NO₂.³³ These studies show that chemical reactivity is dependent on the Nb cluster size and its charge. To supplement the experimental work on Nb clusters, ab initio methods and density functional theory (DFT) have investigated the geometries and electronic states of Nb_x clusters and their adducts with nitrogen.^{34,35} In this work, we investigate the structure and bonding patterns in Nb⁺(N₂)_{1–16} complexes with infrared photodissociation spectroscopy and DFT calculations.

Our recent study of the infrared spectroscopy of V⁺(N₂)_n was the first that probed the N–N stretch of an isolated TM⁺(N₂) complex and thereby confirmed its structure and ground electronic state.³⁶ Until recently, such studies were not possible due to the limited availability of suitable infrared laser sources. However, utilizing IRPD and a new optical parametric oscillator/amplifier (OPO/OPA) laser system, we have been able to obtain infrared spectroscopy for a variety of metal cation–molecular complexes such as M⁺(CO)₂, M⁺(C₂H₂)_n, M⁺(H₂O)_n, and M⁺(C₆H₆)_n.^{37–41} These studies have provided the structures and other bonding parameters of these gas-phase metal ion com-

plexes. Unlike ligands such C₂H₂ and H₂O, N₂ does not have an IR active mode in the gas phase. However, as demonstrated by our work with V⁺(N₂)_n,³⁶ nitrogen binding to a TM⁺ does “switch-on” the IR activity of the N–N stretch (due to the reduced symmetry of the TM⁺–N₂ complex), and its intensity is easily detectable. Both V⁺ and Nb⁺ have low-lying quintet and triplet atomic states, and it is interesting to investigate which of these will be most important in ligand binding. N₂ is isoelectronic to CO but binds more weakly to transition metals, making its coordination behavior more varied. A number of neutral TM–N₂ complexes have been synthesized or produced in matrix isolation experiments and studied with infrared spectroscopy.⁴² Their N–N stretching frequencies fall in the 2000–2300 cm^{−1} region. The infrared spectra obtained here provide an in-depth probe of the coordination and structures for gas-phase ionic complexes of niobium, as well as the role of high-spin versus low-spin electronic configurations in ligand bonding for these systems.

Experimental Section

The apparatus and methods employed here have been described previously.⁴¹ The Nb⁺(N₂)_n complexes were produced in a pulsed nozzle cluster source by ablating a 0.5-in. Nb rod with the focused output of a Nd:YAG laser at 355 nm. A general valve (series 9) operating with a backing pressure of 70–80 psi and pulse duration of 260–280 μs was employed to generate pure nitrogen expansions that led to cluster growth. The expansion was skimmed into a differentially pumped reflectron time-of-flight mass spectrometer where positive pulses applied to the acceleration plates injected the cation complexes into the first drift tube. The ions of interest were then mass-selected by their flight time with pulsed deflection plates. The size-selected ions entered the reflectron region where they slowed, turned, and then reaccelerated into the second drift tube. At the turning point in the reflectron, the ions were excited with tunable IR laser radiation from a Nd:YAG pumped optical parametric oscillator/amplifier (OPO/OPA, LaserVision) to induce resonance-enhanced dissociation. Scans were conducted in the wavelength region of 2100–2500 cm^{−1}; the OPO laser system used for this experiment did not provide IR with good efficiency below 2100 cm^{−1}. The parent and fragment ions produced by photodissociation accelerated into the second drift region, after which an electron multiplier tube detector in conjunction with a LeCroy WaveRunner LT-342 digital oscilloscope detected them. The signal was transferred to a PC computer via an IEEE-488 interface. Monitoring the fragment yield as a function of the laser wavelength generated an IR excitation spectrum of each parent ion.

DFT was used to compute the structures, energetics, and spectra of the small Nb⁺(N₂)_n complexes for comparison to the experiment. The Nb⁺(N₂)_{1–6} complexes were investigated using the B3LYP functional in the Gaussian 03W package.⁴³ The Gaussian basis set in DGAUSS (DG) that is double-ζ valence plus polarization (DZVP) and then indicated as DGDZVP was employed for Nb⁺, while the 6-311+G* basis set was used to describe nitrogen. All calculations allowed for symmetry breaking, and multiple spin states were considered for each initial geometry. The computed vibrational frequencies were scaled by a factor

- (24) Siegbahn, P. E. M.; Blomberg, M. R. A. *Annu. Rev. Phys. Chem.* **1999**, *50*, 221.
 (25) Armentrout, P. B. *Int. J. Mass Spectrom.* **2003**, *227*, 289.
 (26) (a) Langhoff, S. R.; Petterson, L. G. M.; Bauschlicher, C. W., Jr.; Partridge, H. *J. Chem. Phys.* **1987**, *86*, 268. (b) Bauschlicher, C. W., Jr.; Langhoff, S. R.; Partridge, H.; Barnes, L. A. *J. Chem. Phys.* **1989**, *91*, 2399. (c) Barnes, L. A.; Rosi, M.; Bauschlicher, C. W., Jr. *J. Chem. Phys.* **1990**, *93*, 609. (d) Sodupe, M.; Bauschlicher, C. W., Jr. *J. Phys. Chem.* **1991**, *95*, 8640. (e) Bauschlicher, C. W., Jr.; Partridge, H.; Sheehy, J. A.; Langhoff, S. R.; Rosi, M. *J. Phys. Chem.* **1992**, *96*, 6969.
 (27) (a) Carroll, J. J.; Haug, K. L.; Weisshaar, J. C. *J. Am. Chem. Soc.* **1993**, *115*, 6962. (b) Carroll, J. J.; Haug, K. L.; Weisshaar, J. C.; Blomberg, M. R. A.; Siegbahn, P. E. M.; Svensson, M. *J. Phys. Chem.* **1995**, *99*, 13955.
 (28) (a) Eller, K.; Schwarz, H. *Chem. Rev.* **1991**, *91*, 1121. (b) Schwarz, H. *Int. J. Mass Spectrom.* **2004**, *237*, 75.
 (29) Sievers, M. R.; Chen, Y. M.; Haynes, C. L.; Armentrout, P. B. *Int. J. Mass Spectrom.* **2000**, *195/196*, 149.
 (30) (a) Kim, Y. D.; Gantefor, G. *Chem. Phys. Lett.* **2003**, *382*, 644. (b) Kim, Y. D.; Gantefor, G. *J. Mol. Struct.* **2004**, *692*, 139.
 (31) Mwakapumba, J.; Ervin, K. M. *Int. J. Mass Spectrom. Ion Processes* **1997**, *161*, 161.
 (32) Berces, A.; Hackett, P. A.; Lian, L.; Mitchell, S. A.; Rayner, D. M. *J. Chem. Phys.* **1998**, *108*, 5476.
 (33) Wu, Q.; Yang, S. *Int. J. Mass Spectrom.* **1999**, *184*, 57.
 (34) Sellers, H. *J. Phys. Chem.* **1990**, *94*, 1338.
 (35) Berces, A.; Mitchell, S. A.; Zgierski, M. Z. *J. Phys. Chem. A* **1998**, *102*, 6340.
 (36) Pillai, E. D.; Jaeger, T. D.; Duncan, M. A. *J. Phys. Chem. A* **2005**, *109*, 3521.
 (37) (a) Gregoire, G.; Duncan, M. A. *J. Chem. Phys.* **2002**, *117*, 2120. (b) Jaeger, J.; Jaeger, T.; Duncan, M. A. *Int. J. Mass Spectrom.* **2003**, *228*, 285. (c) Walker, N. R.; Walters, R. S.; Grieves, G. A.; Duncan, M. A. *J. Chem. Phys.* **2004**, *121*, 10498. (d) Walker, N. R.; Walters, R. S.; Duncan, M. A. *J. Chem. Phys.* **2004**, *120*, 10037.
 (38) (a) Walters, R. S.; Jaeger, T. D.; Duncan, M. A. *J. Phys. Chem. A* **2002**, *106*, 10482. (b) Walters, R. S.; Schleyer, P. v. R.; Duncan, M. A. *J. Am. Chem. Soc.* **2005**, *127*, 1100. (c) Walters, R. S.; Pillai, E. D.; Schleyer, P. v. R.; Duncan, M. A. *J. Am. Chem. Soc.* **2005**, *127*, 17030.

- (39) (a) Walker, N. R.; Walters, E. D.; Pillai, E. D.; Duncan, M. A. *J. Chem. Phys.* **2003**, *119*, 10471. (b) Walters, R. S.; Duncan, M. A. *Aust. J. Chem.* **2004**, *57*, 1145. (c) Walker, N. R.; Walters, R. S.; Tsai, M.-K.; Jordan, K. D.; Duncan, M. A. *J. Phys. Chem. A* **2005**, *109*, 7057.
 (40) (a) Jaeger, T. D.; Pillai, E. D.; Duncan, M. A. *J. Phys. Chem. A* **2004**, *108*, 6605. (b) Jaeger, T. D.; Duncan, M. A. *J. Phys. Chem. A* **2005**, *109*, 3311.
 (41) (a) Duncan, M. A. *Annu. Rev. Phys. Chem.* **1997**, *48*, 69. (b) Duncan, M. A. *Int. Rev. Phys. Chem.* **2003**, *22*, 407.
 (42) Nakamoto, K. *Infrared and Raman Spectra of Inorganic and Coordination Compounds*, 5th ed.; Wiley: New York, 1997; Part B, pp 173–176.
 (43) Frisch, M. J.; et al. *Gaussian 03*, revision B.02; Gaussian, Inc.: Pittsburgh, PA, 2003.

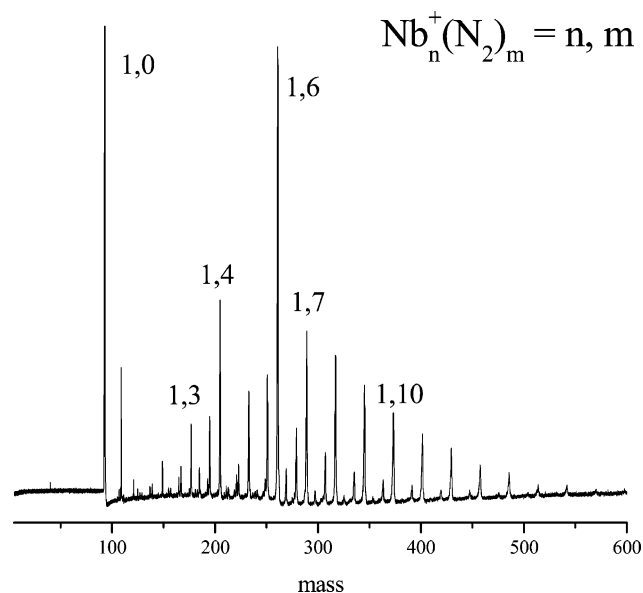


Figure 1. Mass spectrum of $\text{Nb}^+(\text{N}_2)_n$ complexes produced in this experiment.

of 0.96, which is the recommended value for the B3LYP/6-311+G* method.^{44,45} With this correction, the free N_2 molecule frequency was calculated to be 2359 cm^{-1} , which was slightly higher than the well-known experimental value for the fundamental frequency of N_2 at 2330 cm^{-1} ($\omega_e = 2358.6\text{ cm}^{-1}$).⁴⁶ Energies are reported without zero-point corrections, as this correction was not likely to be straightforward in these complexes with low frequency bending modes that may be subject to large anharmonicities. No systematic study of different basis sets or functionals was attempted, as those indicated have been employed in many previous studies of transition-metal complexes.⁴⁷ Likewise, the methods used did not allow spin-orbit interaction to be included in these calculations.

Results and Discussion

The mass spectrum of $\text{Nb}^+(\text{N}_2)_n$ complexes produced in this experiment is shown in Figure 1. It is similar to the one presented for $\text{V}^+(\text{N}_2)_n$ in our previous work,³⁶ with complexes produced for $\text{Nb}^+(\text{N}_2)_n$ up to $n = 15$. This spectrum shows that complexes are produced by the addition of intact N_2 molecules around the metal ion with no evidence for ligand fragmentation. The intermediate masses in the figure are mixed complexes of the form $\text{Nb}^+(\text{N}_2)_n(\text{H}_2\text{O})_m$ resulting from water added to the expansion gas to improve the yield of complexes.⁴¹ As shown, there is a noticeably enhanced intensity for the $n = 6$ mass channel, and a secondary maximum in intensity for the $n = 4$ mass channel. These intensity maxima are often indicative of the preferred coordination for the metal cation, which we investigate further below. We expect that there will be a “core” of more strongly bound ligands interacting directly with the metal cation, and because of the supersonic cooling in the experiment, more weakly bound external ligands can attach to the exterior of this core via van der Waals forces. To explore these clustering dynamics, we investigate the vibrational spectroscopy of these complexes as a function of their size. We excite each mass-selected complex near the N–N stretch of free

N_2 (2330 cm^{-1}),⁴⁶ and because the ion density is too low for absorption spectroscopy, we measure resonance-enhanced photodissociation spectra to reveal the infrared spectra.

IR excitation in the N–N stretch region of $\text{Nb}^+(\text{N}_2)_n$ for $n = 1–3$ produces little or no dissociation. Although these cluster sizes are present in high abundance, their photofragmentation yields are quite low. Starting with the $n = 4$ complex, the fragmentation yield for the loss of N_2 molecules increases, enabling us to measure IR photodissociation spectra in the $2100–2500\text{ cm}^{-1}$ region with good signals. We have observed a similar trend in other TM–ligand systems, where no dissociation is observed for the smallest complexes because of their stronger ligand bonding.^{36–41} The IR photons corresponding to vibrational fundamentals simply do not have enough energy to break the weakest bond in the complex (i.e., the TM^+ –ligand bond). As cluster size increases, the bonding capacity of the TM cation is distributed to the additional ligands, and this usually reduces the per-bond dissociation energy. Eventually, IR photons are sufficiently energetic to eliminate at least one ligand from the complex.

To test these ideas for the $\text{Nb}^+(\text{N}_2)_n$ system, we would like to know the metal–ligand bond energies for the different sized complexes. However, these have not been measured, and therefore we employed DFT to calculate them. The essential results of the calculations are presented in Table 1, while a full description of the results are given in the Supporting Information. Although the B3LYP method is well-known to have limited accuracy for dissociation energies, it is sometimes useful to derive trends in energies for different clusters.⁴⁷ However, the B3LYP results here predict that the dissociation energy for all of the small $\text{Nb}^+(\text{N}_2)_n$ complexes ($n = 1–6$) is more than 17 kcal/mol ($\sim 6000\text{ cm}^{-1}$). If we believe this, excitation of the N_2 stretch could not fragment any of these small complexes unless a multiphoton process occurs, and such processes are inefficient with our infrared laser intensities ($5–7\text{ mJ/pulse}$ in a 3-mm diameter spot). Because we do indeed measure fragmentation beginning at about $n = 3$, we conclude that the binding energies are actually much lower than the values computed, and that DFT/B3LYP is problematic for the quantitative binding energies in this system. We found similar behavior for $\text{V}^+(\text{N}_2)_n$ complexes.³⁶

Figure 2 shows the fragmentation mass spectra for the $n = 6–9$ complexes acquired by tuning the IR OPO to a wavelength of 2215 cm^{-1} . These data are obtained by a computer difference method (fragmentation laser “on”–“off”), where the negative peaks correspond to the depletion of the selected parent ion and the positive peaks to the photofragments. These spectra show that photodissociation proceeds by the elimination of intact N_2 molecules. In data not shown, the complexes smaller than $n = 6$ all fragment (less efficiently) by the loss of a single N_2 molecule. Likewise, the $n = 6$ complex also dissociates by losing one N_2 molecule. Beginning with the $n = 7$ complex and extending out to $n = 9$ (and beyond), the complexes eliminate single or multiple N_2 molecules, with the sequence of ligand eliminations terminating at the cluster size of $n = 6$. Such a common termination point in fragmentation has been observed previously for other TM^+ –ligand complexes.^{36–41} Ligands that are attached directly to the TM cation, forming the coordination “core”, are more strongly bound than the external ones, and these resist elimination in the photodisso-

(44) Scott, A. P.; Radom, L. *J. Phys. Chem.* **1996**, *100*, 16502.

(45) Anderson, M. P.; Uvdal, P. *J. Phys. Chem. A* **2005**, *109*, 2937.

(46) Huber, K. P.; Herzberg, G. *Molecular Spectra and Molecular Structure*; Prentice Hall: New York, 1979; Vol. 4.

(47) Klippenstein, S. J.; Yang, C. N. *Int. J. Mass Spectrom.* **2000**, *201*, 253.

Table 1. Results of Theory for the Quintet and Triplet Electronic States of $\text{Nb}^+(\text{N}_2)_n$ Complexes^a

n	structure	relative energy	BE	D _e	IR frequency (cm ⁻¹) (oscillator strength, km/mol)
1	L(⁵ Σ) (σπ ² σ)	0.0	17.0	17.0	2265(58)
	T(⁵ B ₁) (a ₁ b ₂ a ₂ a ₁)	+14.1	2.9	2.9	2212(95)
	L(³ Σ) (σ ² π ²)	+43.7	3.4	3.4	2191(164)
	T(³ A ₂) (a ₂ b ₂ ² a ₁)	+22.7	24.3	24.3	1795(169)
2	L(⁵ Σ _g) (π _g ² δ _g ²)	0.0	42.4	25.4	2244(383)
	LT(⁵ A ₁) (b ₂ b ₁ a ₂ a ₁)	+13.7	28.7	25.8, 11.7 ^b	2216(221), 2247(101)
	T(³ A _g) (b ₃ b ₂ b ₁ g _g)	+28.8	13.6	10.7	2221(252)
	L(³ Σ _g) (σ _g ² π _g ²)	+18.0	54.4	51.1	2188(732)
	LT(³ B ₁) (a ₁ b ₁ b ₂ ²)	+28.1	44.5	20.2, 41.2 ^b	2033(505), 2220(205)
	T(³ B ₂) (a ₂ ² b ₂ a ₁)	+36.7	35.7	11.3	1992(848), 2044(3)
3	L(⁵ A ₁) (b ₂ a ₂ b ₁ a ₁)	0.0	61.1	18.7	2226(165), 2251(317)
	L(³ B ₂) (b ₁ a ₂ b ₂ ²)	+11.5	79.6	25.1	2171(310), 2197(661)
4	L(³ B ₂ g) (b ₂ g _g e _g e _g a ₁ g)	0.0	79.5	18.4	2251(336), 2251(336)
	L(³ A ₁ g) (e _g e _g b ₂ g ²)	+8.4	101.1	21.5	2209(605), 2209(605)
5	L(³ A) (a ² aa)	0.0	122.5	21.4	2203(158), 2208(609)
					2210(148), 2217(536)
	L(⁵ B ₁) (b ₁ ee _g)	+10.8	81.7	2.2	2235(400), 2235(400)
6					2257(15), 2321(4)
	L(³ B _g) (a _g ² b _g a _g)	0.0	140.8	18.5	2225(472), 2225(459)
					2227(539)

^a Relative energies, binding energies [relative to separated Nb^+ (⁵D and ³P, respectively) and $n\text{N}_2$], dissociation energies for the process $\text{Nb}^+(\text{N}_2)_n \rightarrow \text{Nb}^+(\text{N}_2)_{n-1}$, predicted frequencies, electronic configurations, and IR oscillator strengths for the calculated structures shown in Figure 5. Frequencies were scaled by 0.96. All energies are in kilocalories per mole. L and T indicate end-on and side-on ligand binding configurations, respectively. ^b For removal of the T-configured ligand.

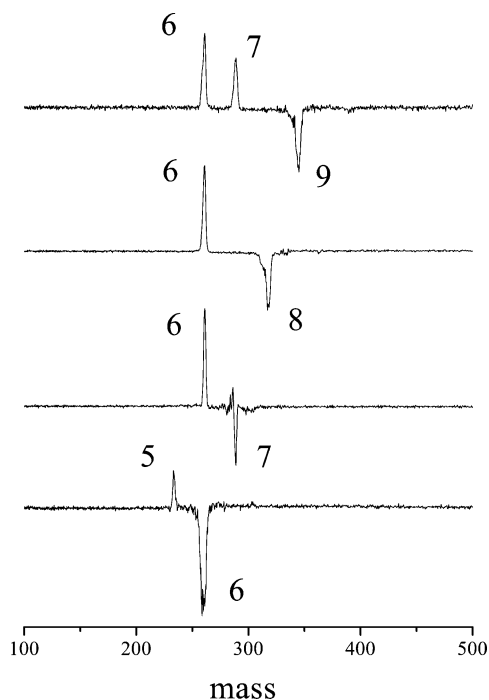


Figure 2. Fragmentation mass spectra for $\text{Nb}^+(\text{N}_2)_{6-9}$ complexes. The complexes fragment by the loss of intact N_2 molecules, and the larger complexes terminate at $n = 6$.

ciation process. As we have discussed before, the surviving complex of the cation and its more strongly bound ligands provides an indication for the coordination number of the TM cation.³⁶⁻⁴¹ In the case of Nb^+ , these fragmentation spectra indicate a coordination of six nitrogen molecules, which is the Nb^+ cation's favored coordination in the condensed phase as well.⁹ This is also consistent with the enhanced intensity for the $\text{Nb}^+(\text{N}_2)_6$ peak in the mass spectrum of complexes produced by the source. Although an enhanced intensity in the mass spectrum was also noted above at $n = 4$, and a coordination of $n = 4$ is also known for many transition-metal cations, there is

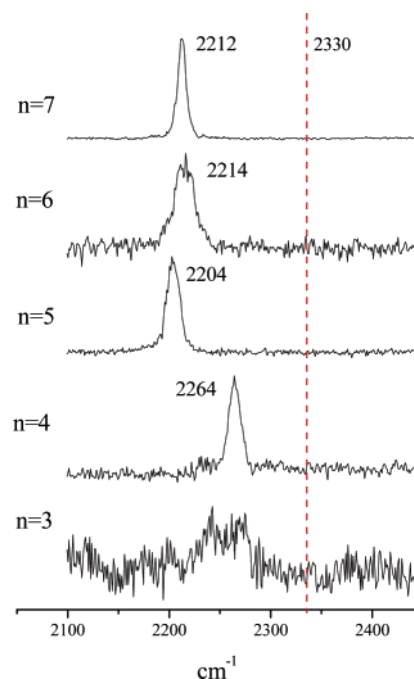


Figure 3. IRPD spectra for $\text{Nb}^+(\text{N}_2)_n$, $n = 3-7$ acquired by monitoring the loss of N_2 as a function of OPO wavelength. The dashed vertical line indicates the frequency of the N–N stretch in free N_2 .

no evidence in these breakdown patterns for a special stability of this complex relative to its neighbors.

The wavelength dependence of the IR photodissociation processes for $\text{Nb}^+(\text{N}_2)_n$, $n = 3-7$ is shown in Figure 3. As illustrated, resonances are detected for each of these clusters in their dissociation yields. As seen previously, binding to the cation does activate the N–N stretch, making it possible to obtain spectra with good intensities for the larger complexes. Consistent with this, the DFT calculations also indicate substantial IR intensities for the vibrations in these complexes. The spectra here are acquired by monitoring the dissociation yield of the parent ion as a function of the IR wavelength. For those

ions with multiple fragments, each channel was measured to see if the spectra were different. In each case, all channels for a particular parent signal produced spectra differing only in the signal level. The spectrum presented in Figure 3 for each cluster size is therefore the one that carries the greatest signal. As discussed above, the complexes for $n = 1-3$ have low fragmentation yields, producing spectra with low signal levels. The $n = 3$ complex has a barely discernible resonance around 2250 cm^{-1} . The spectra for $n = 4-7$ complexes each have a single band in the region between 2200 and 2300 cm^{-1} . Larger complexes up to $n = 16$ have essentially the same spectrum as the $n = 7$ species. A few of these have an additional weaker feature near 2338 cm^{-1} , as discussed below.

The dashed line in Figure 3 indicates the fundamental frequency of free N_2 at 2330 cm^{-1} . It is therefore apparent that all of the resonances in these spectra are shifted to the red by about $60-120 \text{ cm}^{-1}$ from this frequency. The significant red-shifts seen here agree qualitatively with the predictions of the Dewar–Chatt–Duncanson (DCD) complexation model.⁴⁸ This model considers the TM–ligand bond as a synergistic mix of σ -type donation of electron density from the ligands into the empty TM d-orbitals and π -type back-donation from the TM orbitals into the antibonding orbitals of the ligand. Such a mechanism weakens the bonding in nitrogen, lowering its vibrational frequency in much the same way that the CO stretch usually shifts to the red in metal carbonyl complexes.^{10,12} In metal carbonyls, this shift is large enough so that the CO frequency is usually found below 2000 cm^{-1} .^{10,12} The red-shifts seen here for $\text{Nb}^+(\text{N}_2)_n$ (and those found earlier for $\text{V}^+(\text{N}_2)_n$ complexes)³⁶ are smaller than this. However, these N–N stretching frequencies do fall in the range noted previously for stable N_2 complexes synthesized or for those studied in matrix isolation experiments.^{21,42}

The $n = 3$ complex has barely enough dissociation so that a discernible resonance can be detected near 2250 cm^{-1} . Beginning with $\text{Nb}^+(\text{N}_2)_4$, the dissociation yields are higher and we obtain IR spectra with relatively strong bands. For $n = 4$, there is a single band at 2264 cm^{-1} , which is shifted to the red by 66 cm^{-1} compared to the resonance in the free N_2 molecule. The $n = 5$ complex also has a single peak that is centered at 2204 cm^{-1} . This is a shift of 60 cm^{-1} further to the red from the $n = 4$ resonance and a total of 126 cm^{-1} from free nitrogen. The spectra for the $n = 6$ and 7 complexes also contain single bands, which are slightly less red-shifted than the $n = 5$ band. $\text{Nb}^+(\text{N}_2)_6$ has a single feature at 2214 cm^{-1} that lies 116 cm^{-1} to the red from free N_2 . The single peak for $\text{Nb}^+(\text{N}_2)_7$ falls at 2212 cm^{-1} , which is 118 cm^{-1} lower than the free- N_2 resonance. Table 2 summarizes these band positions and lists those for the larger clusters that we have studied but are not shown here. The larger clusters all have a single band at essentially the same position as that of the $n = 7$ complex. It is interesting to note that the spectrum for $\text{Nb}^+(\text{N}_2)_6$ has a lower signal level and a broader peak width than the other complexes in the $n = 4-7$ range. On the basis of our results from the fragmentation mass spectra, we have shown that Nb^+ prefers a coordination of six in these complexes. Because of this, the $n = 6$ complex should perhaps be harder to dissociate than the $n = 5$ and 7 complexes, thus explaining the lower signal levels. Additional width for

Table 2. Vibrational Band Positions Measured for the Studied $\text{Nb}^+(\text{N}_2)_n$ Complexes

n	frequency (cm^{-1})	n	frequency (cm^{-1})
1		9	2212
2		10	2212
3	2240, 2270	11	2210, 2338
4	2264	12	2210, 2338
5	2204	13	2210
6	2214	14	2209
7	2212	15	2209, 2338
8	2212	16	2208

this band is also consistent with this, because the fraction of warmer clusters present in the beam gains an advantage in dissociation when other energetics are marginal. Such warm clusters would have a broader rotational profile.

The mass spectrum in Figure 1, the fragmentation data in Figure 2, and the lower fragmentation efficiency for the $n = 6$ complex in Figure 3 are all consistent with a coordination number of six for these complexes. If this is true, then the seventh N_2 molecule in the cluster, and all subsequent ones, should be bound by only $(\text{N}_2)-(\text{N}_2)$ interactions. These outer ligands should perhaps have binding energies close to that of the van der Waals $(\text{N}_2)_2$ dimer. The nitrogen dimer has been investigated theoretically and spectroscopically.⁴⁹⁻⁵¹ Its equilibrium structure is T-shaped, with a binding energy of $50-100 \text{ cm}^{-1}$. If outer ligands are bound with energies such as this, they should be eliminated easily by photoexcitation. Indeed, the $n = 7$ complex and all larger ones dissociate efficiently, producing spectra with high signal levels. However, this view is perhaps oversimplified because the inner-sphere N_2 ligands are expected to be polarized by their interaction with the metal, thus enhancing their binding interactions with second-sphere molecules. Apparently, such an induced polarization leads to an (inner N_2)–(outer N_2) interaction that is still weak compared to the photon energy. The outer N_2 ligands are expected to vibrate at frequencies close to that of the free N_2 molecule or to the frequency of N_2 in its van der Waals dimer (both occur at 2330 cm^{-1}). However, this vibration is expected to be only weakly IR active (if at all) in these outer molecules, because they have no dipoles and do not interact significantly with the metal ion. Consistent with this, there is hardly any detectable signal near the free molecule resonance that might be assigned to external N_2 for any of the clusters for $n \geq 7$. The exceptions to this occur for some clusters in the much higher size range ($n = 11, 12, 15$). As an example, Figure 4 shows the spectra for the $n = 11$ and 12 complexes, where such a weak band is present at about 2338 cm^{-1} .

DFT calculations were also employed to investigate these infrared spectra. Studies were completed only for the $n = 1-6$ species. Geometrical convergence was quite difficult to obtain for the $n = 6$ species, and because larger complexes would have weaker van der Waals ligands (not expected to be handled well by DFT), we did not extend calculations beyond this. Figure 5 shows the optimized lowest-energy structures for each of these small clusters, while the predicted IR active frequencies, oscillator strengths, electronic states, binding energies, and dissociation energy (D_e) for the removal of the last ligand are

(48) (a) Chatt, J.; Rowe, G. A.; Williams, A. A. *Proc. Chem. Soc., London*, **1957**, 208. (b) Chatt, J.; Duncanson, L. A.; Guy, R. G. *J. Chem. Soc.* **1961**, 827.

(49) Long, C. A.; Henderson, G.; Ewing, G. E. *Chem. Phys.* **1973**, *2*, 485.

(50) Couronne, O.; Ellinger, Y. *Chem. Phys. Lett.* **2000**, *306*, 71.

(51) Aquilanti, V.; Bartolomei, M.; Cappelletti, D.; Carmona-Novillo, E.; Pirani, F. *J. Chem. Phys.* **2002**, *117*, 615.

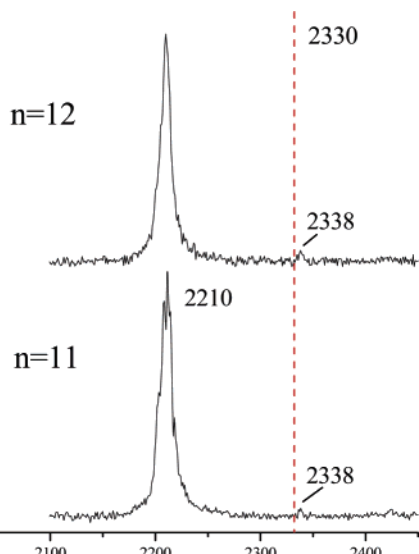


Figure 4. IRPD spectra for $\text{Nb}^+(\text{N}_2)_{11}$ and $\text{Nb}^+(\text{N}_2)_{12}$ showing the weak resonance at 2338 cm^{-1} attributed to external N_2 molecules not interacting directly with the metal.

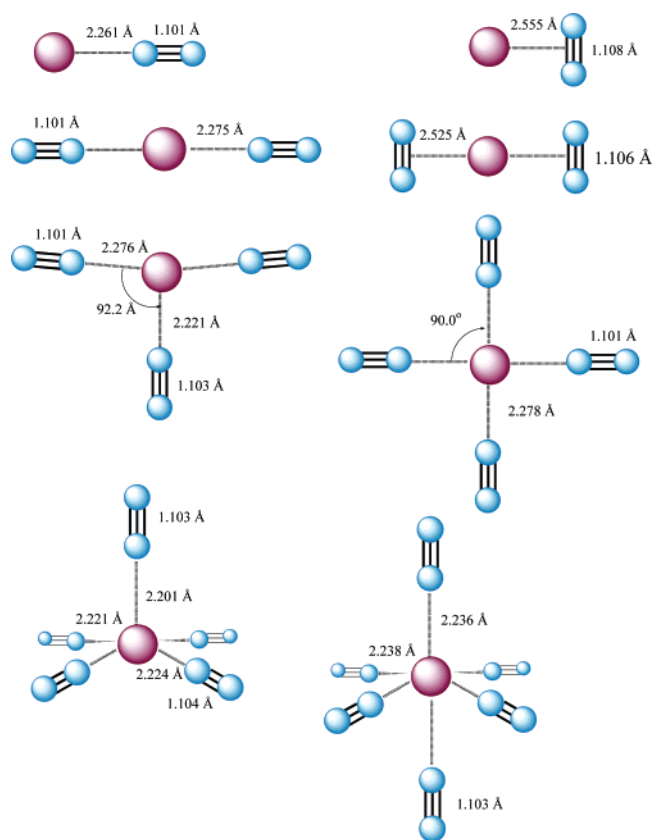


Figure 5. Lowest-energy structures for $\text{Nb}^+(\text{N}_2)_n$, $n = 1-5$ computed using the B3LYP functional.

listed in Table 1. The ground state of Nb^+ is d^4 (^5D), and its first excited state is d^4 (^3P), which lies experimentally about 16 kcal/mol higher in energy. However, this energy difference is exaggerated by DFT, which finds an atomic spacing of 30 kcal/mol. This discrepancy for the atomic splitting results because a single configuration is not adequate to represent the excited triplet state, but this problem is expected to be greatly reduced in the molecular complexes. It is well-known that second-row transition metals possess low-lying excited states that may bind

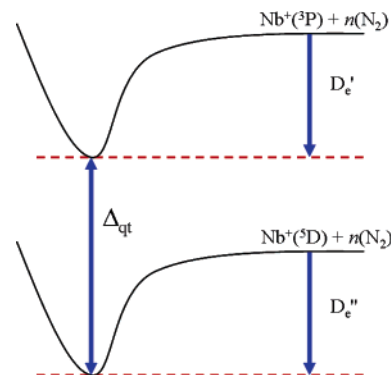


Figure 6. Schematic diagram showing the bonding energetics of Nb^+ in its ground (^5D) state versus its excited (^3P) state. D_e' is the binding in the quintet metal state, while D_e'' is the binding in the metal triplet state. Δ_{qt} is the energy difference between the complexes in these two spin states.

ligands more strongly than the ground state,^{12,26} and therefore in each complex and geometry we explored both the high-spin quintet and low-spin triplet states of Nb^+ . The dissociation energies presented here are relative to the respective atomic state of the metal with that same spin. Figure 6 shows a schematic of these energetics, including the binding energy of the complex relative to the quintet metal asymptote (D_e') and that relative to the triplet metal asymptote (D_e''). As noted below, these binding energies vary significantly from one complex to another. Figure 6 also indicates the quintet–triplet energy difference in the complex, which is defined as Δ_{qt} .

Because the multireference problem in the excited d^4 (^3P) state of Nb^+ affects the relative binding energies of quintet states versus their corresponding triplets, it is difficult to decide how to report the dissociation energies and Δ_{qt} values for the complexes studied here. The version of DFT in Gaussian that we use cannot handle the different configurations that give rise to the excited triplet state, and this results in the gross overestimation of the atomic spacing for the ground d^4 (^5D) versus d^4 ($^3\text{P}_{0,1,2}$) state. The same problem occurs in the splittings for the corresponding states of the $\text{Nb}^+(\text{N}_2)_n$ complexes, but to a significantly lesser degree. Therefore, if we forced the atomic $^5\text{D}-^3\text{P}$ spacing to the experimental value, and then shifted the other energetics relative to this, all the quintet–triplet splittings in the complexes would be overcorrected to values that are too small. Although the multireference problem is expected to be smaller in the molecular species, there is no systematic way to correct for the exact unknown amount of error here. We therefore report the energy differences as calculated for the molecules and reference these to the (incorrect) computed value for the atomic splittings. In addition, the d^4 ($^3\text{P}_{0,1,2}$) excited state consists of three spin–orbit multiplet components located experimentally at 5562, 6192, and 7261 cm^{-1} . Our DFT methods do not distinguish these multiplets, which are spread over about 1700 cm^{-1} (about 5 kcal/mol) of energy. Because we do not correct the DFT value for the actual atomic splitting, we have also ignored these spin–orbit splittings. By these choices, it is clear that quantitative energetics cannot be trusted for either the dissociation energies of these complexes or their quintet–triplet energy splittings. However, previous work on similar systems has shown that *relative* energetics in such a framework are still useful.⁴⁷ We therefore proceed with due caution, recognizing the limitations inherent in these DFT calculations.

The $n = 1$ species demonstrates the issues that arise throughout the calculations for the different sized complexes. Two minima are found for each spin state, corresponding to “end-on” and “side-on” binding configurations of the N_2 molecule to Nb^+ . The linear structure (L complex, end-on binding) for the quintet state lies lowest in energy overall and is more strongly bound by 14 kcal/mol than the next-best T-shaped (T complex, side-on binding) quintet complex. The excited triplet state in the T configuration forms a bond (relative to its excited asymptote) stronger than that of the linear quintet ground state. However, if we look at the Δ_{qt} values, we can see that the quintet is still apparently the overall lowest-energy configuration. If we compare only the linear structures, the Δ_{qt} value is 43.7 kcal/mol, but this is not really a fair comparison. However, if we compare the “best” triplet (T-shaped) to the “best” quintet (linear), the Δ_{qt} value is 22.7 kcal/mol, and therefore the L quintet is favored as the overall ground state.

For all of the electronic states and binding configurations for the $n = 1$ complex, DFT predicts a lower N–N stretch vibration compared to free N_2 , in accordance with the DCD model. In the quintet state, the linear and T-shaped complexes are predicted to red-shift by 65 and 118 cm^{-1} , respectively. The triplet state red-shifts are predicted to be 139 and 535 cm^{-1} for the linear and T-shaped complexes, respectively. Two trends emerge from the predicted frequencies. For a given electronic state, the T-shaped complex results in a greater red-shift than the corresponding linear complex since the TM^+ binds directly to the π -bond, perturbing the N–N bonding to a greater extent. Second, for a given N_2 binding configuration, the triplet state of Nb^+ red-shifts the N_2 frequency more than the quintet state. Previous studies on first- and second-row systems indicate that a TM–ligand bond formed via a low-spin state usually possesses larger covalent character than one formed by a high-spin state.^{12,26} As a result, the lower-spin state causes a greater perturbation of the ligand, consistent with our DFT results here.

For the $n = 2$ complex, a thorough search of the potential energy surface for each spin state was performed. For each spin state, minimum energy geometries were located for both N_2 binding in an end-on configuration (2L complex), one end-on and one side-on (L–T complex), and both side-on (2T complex). For the 2T complex, the quintet D_{2h} and D_{2d} structures are saddle points and only a triplet C_{2v} (distorted with two metal–ligand planes about 10° from D_{2h}) structure is a minimum. For the quintet minima, the 2L complex has a greater binding energy than the L–T complex. A similar trend is observed for the triplet state. In contrast to the trend for the $n = 1$ complex, the 2L triplet configuration is much more strongly bound than the 2T. Additionally, it is apparent that the second ligand in this 2L triplet state is remarkably more strongly bound than the first (D_e of 51.1 versus 3.4 kcal/mol). Many examples of such behavior have been documented for other transition-metal complexes,¹² but the magnitude of this effect is surprisingly large here. On the other hand, the 2T triplet has the opposite trend, where the second ligand is slightly more weakly bound than the first. The L–T complex again has two values for D_e and frequencies that correspond to the L and T ligands. However, here the larger D_e (41.2 kcal/mol) corresponds to the loss of the “side-on” N_2 since the T-shaped $n = 1$ isomer is more strongly bound than the linear isomer in the triplet state. The overall lowest energy for the $n = 2$ complex is for the 2L quintet

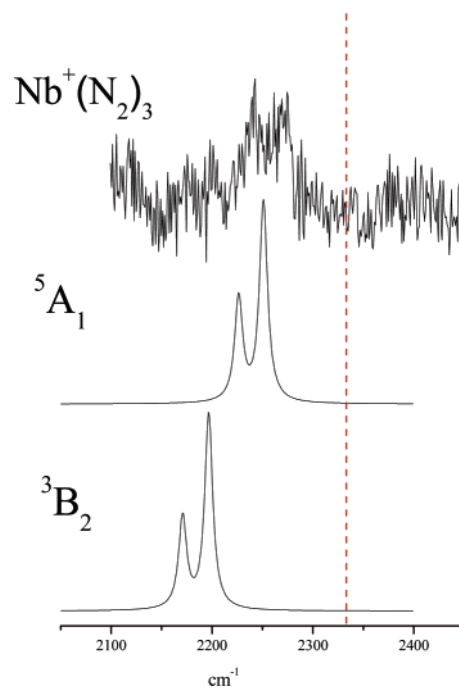


Figure 7. Comparison of the vibrational spectrum measured for $\text{Nb}^+(\text{N}_2)_3$ to the predictions of theory for complexes in either quintet or triplet spin states.

species. Comparing this to the lowest triplet (also 2L) gives a splitting of $\Delta_{\text{qt}} = 18.0$ kcal/mol. This is significantly smaller than the value (43.7 kcal/mol) for the linear $n = 1$ complex and somewhat smaller also than the value for the best triplet versus best quintet structures (22.7 kcal/mol). Beginning a trend that continues in the larger clusters, the second ligand reduces the quintet–triplet splitting compared to the $n = 1$ complex because of the more favorable binding to the excited (low-spin) metal.

Beginning with $n = 3$, the number of possible L–T isomers increases significantly, but as shown for the $n = 2$ species, such complexes would have at least two distinct IR frequencies that would be resolvable by our experiment. However, with the possible exception of the $n = 3$ species, we observe only a single band for all the complexes, suggesting that all the N_2 molecules bind in equivalent orientations. Therefore, for complexes larger than $n = 2$, we have not performed calculations on all possible isomers. For $n = 3$, a few selected mixed L–T isomers were investigated, which demonstrate that T configurations are not favorable in the larger clusters. The linear quintet complexes are the most strongly bound for the $n = 1$ and 2 complexes. For $n = 3$, the lowest-energy structure also has all three N_2 molecules binding end-on to Nb^+ but distorted from a trigonal planar structure. Varying the rotational orientation of the axial nitrogen resulted in stationary points much higher in energy. We were unable to locate any minimum for all three N_2 molecules in a “side-on” orientation for either spin state. The quintet state lies lower in overall energy than the triplet state, with a D_e of 18.7 kcal/mol. However, the binding energy in the triplet state relative to its atomic asymptote is again greater than that of the quintet ($D_e = 25.1$ kcal/mol), and this leads to another decrease in Δ_{qt} to 11.5 kcal/mol.

Figure 7 shows a comparison of the calculated spectrum for the $n = 3$ complex to the experimental measurement. Although the signal levels are extremely poor, the IRPD spectrum of the

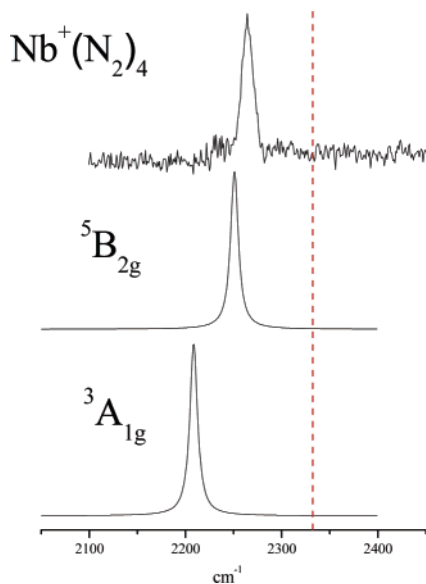


Figure 8. Comparison of the vibrational spectrum measured for $\text{Nb}^+(\text{N}_2)_4$ to the predictions of theory for complexes in either quintet or triplet spin states.

$n = 3$ complex does have broad structure that seems to arise from two bands at about 2240 and 2270 cm^{-1} . The two frequencies of the L quintet are 2226 and 2251 cm^{-1} , whereas the triplet state leads to further red-shifted frequencies at 2171 and 2197 cm^{-1} . As shown, the experimental bands are close to the two predicted for the L quintet complex, but the signal is so low that a more detailed comparison is not possible.

The spectrum of $\text{Nb}^+(\text{N}_2)_4$ with its single peak at 2264 cm^{-1} is indicative of a high-symmetry structure. The only geometries consistent with this are square-planar or tetrahedral structures, and therefore we explored these computationally. The tetrahedral structure does not converge to a stationary point, while the square-planar structure shown in Figure 5 is found to be a minimum for both spin states. Of these, the quintet state is lower in energy by 8.4 kcal/mol. Although Δ_{qt} has decreased even further compared to the smaller complexes, the quintet is still predicted to be the lower energy state here. Figure 8 shows the comparison of the predicted spectra for different spin states to the experiment. The spectrum calculated for the quintet has a single peak centered at 2251 cm^{-1} , which is only 13 cm^{-1} away from the measured band. The corresponding triplet state is predicted to have a band much further to the red at 2209 cm^{-1} . We can therefore conclude that the spectroscopic data and theoretical predictions support a square-planar structure with end-on bonded N_2 molecules in a quintet spin state for the $n = 4$ complex. It is interesting to note that Nb^+ favors this same geometry in the condensed phase.⁹ In general, square-planar structures are most often found for high-spin four-coordinate d^4 complexes.⁹

The spectrum of $\text{Nb}^+(\text{N}_2)_5$ contains a single band at 2204 cm^{-1} , which lies 126 cm^{-1} to the red from the free N_2 stretch. Surprisingly, this band is also shifted about 60 cm^{-1} further to the red from the single band in the $\text{Nb}^+(\text{N}_2)_4$ spectrum. Such an additional red-shift in the spectrum on going from $n = 4$ to larger complexes was also observed in our study of $\text{V}^+(\text{N}_2)_n$.³⁶ To understand this large and unexpected spectral shift between the $n = 4$ and 5 complexes, we consider three different scenarios. A first intriguing possibility is that an *intracuster*

reaction has occurred in the $n = 5$ species, brought about by solvation effects and/or photochemistry. Intracuster reactions have been detected previously by our group for $\text{M}^+(\text{CO}_2)_n$ ($\text{M} = \text{Ni}, \text{V}, \text{Si}$) complexes.³⁷ In $\text{Nb}^+(\text{N}_2)_n$, reaction could lead to TM^+ -nitride species, or perhaps nitrogen ring or metallacycle structures, which seems unlikely because of the high activation energy required to activate the N–N triple bond.^{30–34} There is no evidence in the mass spectrum or fragmentation spectra for the formation of nitrides or for the elimination of nitride fragments. Solvation can promote intracuster reactions if the reaction products are solvated more efficiently than the reactants, but this does not seem to be the case here. Also, in all previous examples of intracuster reactions, only a small fraction of the complexes present reacted. Consequently, the infrared spectra of those systems were much more complex, with multiple bands corresponding to both reacted and unreacted isomers. The single-peak spectrum of $\text{Nb}^+(\text{N}_2)_5$ indicates the presence of only a single structure with high symmetry similar to the $n = 4$ complex. This and the energetic arguments above seem to eliminate the likelihood of any intracuster reactions. Another possibility is that the $n = 5$ species has changed its ligand binding to the side-on configuration. As we note above, side-on or so-called T isomers consistently give rise to larger red-shifts for the N–N stretches in these complexes. Although this would explain a larger red-shift, it would be quite surprising if the $n = 5$ had an *all-T* configuration, when T configurations are unstable for $n = 3$ and when the $n = 4$ complex is completely consistent with an *all-L* configuration. Any mixed L–T isomers would have multiple IR bands, and these are ruled out because the $n = 5$ spectrum has only a single resonance. Our DFT calculations consistently favor end-on over side-on binding, and it also makes sense that T configurations would be less favorable in larger complexes because of the steric crowding of ligands. Thus, a complete switch to T configuration binding for $n = 5$ seems unlikely.

The most likely explanation for the additional band shift in this spectrum is a spin change on the Nb^+ . Figure 9 shows the comparison between theory and experiment, which demonstrates this. The calculated structure for $\text{Nb}^+(\text{N}_2)_5$ with all end-on bound nitrogens is close to a square pyramid, as shown in Figure 5. For the quintet state, the structure has C_{4v} symmetry with IR active frequencies at 2235, 2257, and 2321 cm^{-1} . However, the frequency at 2235 cm^{-1} is a doubly degenerate vibration that is about 50 times more intense than the other bands. As a result, the IR spectrum would be dominated by this single band. The triplet state complex has a similar structure, but its overall symmetry is C_1 and attempts to constrain it to C_{4v} failed. The predicted frequencies are 2203, 2208, 2210, and 2217 cm^{-1} , but only the 2208 and 2217 cm^{-1} vibrations have significant oscillator strengths. When plotted at our experimental line width, the spectrum from these two bands merges into a single feature at 2209 cm^{-1} . As shown in the figure, this predicted band is only 5 cm^{-1} from the measured resonance. Consistent with the spectral shifts, DFT indicates that the addition of the fifth ligand induces a change in the energetic ordering of the spin states, where now the triplet has an energy 10.7 kcal/mol lower than the quintet (i.e., $\Delta_{\text{qt}} = -10.7$). Although DFT is known to misjudge the absolute energies between electronic states with different spins, it usually predicts the vibrational spectrum correctly for a given spin state.⁴⁷ The excellent agreement

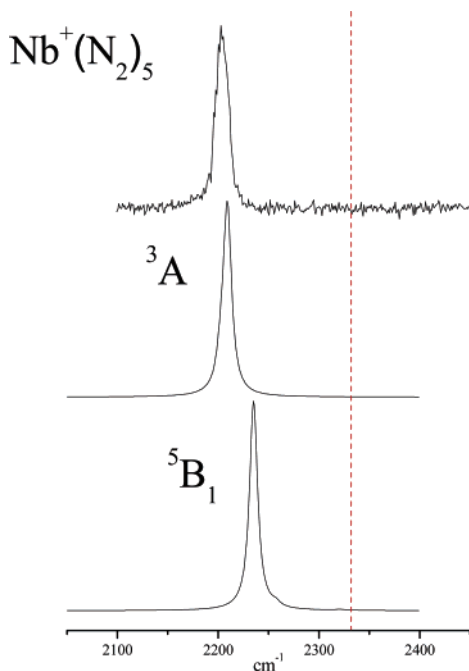


Figure 9. Comparison of the vibrational spectrum measured for $\text{Nb}^+(\text{N}_2)_5$ to the predictions of theory for complexes in either quintet or triplet spin states.

between the theoretical and experimental frequencies, therefore, leads us to conclude that the additional red-shift seen for complexes $n = 5$ (and larger) clusters is due to a spin change on the Nb^+ from quintet to triplet. Changes in metal spin that occur upon progressive addition of ligands have been suggested previously by theory for many transition-metal systems.^{26,52} Likewise, abrupt changes in the reactivities of transition-metal ion complexes that accompany ligand addition have been interpreted to arise from such effects.¹² In particular, a similar spin change has been suggested for the isoelectronic metal V^+ in its $\text{V}^+(\text{H}_2)_n$ complexes upon the addition of the sixth H_2 ligand.^{52,53} However, we believe that this is the first *spectroscopic* confirmation of such an effect in an isolated metal ion complex.

Figure 10 shows the comparison between experiment and theory for the $n = 6$ complex. The peak in the experimental spectrum falls at 2214 cm^{-1} , which is 10 cm^{-1} to the blue of the peak in the $n = 5$ spectrum and 50 cm^{-1} to the red from the band for $n = 4$. Thus, because this band is closer to that in the $n = 5$ spectrum, it is likely that the Nb^+ spin state in $\text{Nb}^+(\text{N}_2)_6$ is also a triplet. The slight difference in band position relative to the $n = 5$ species is likely due to the distribution of binding to six ligands (rather than five), which could reduce the per-ligand interaction and diminish the red-shift. DFT calculations for the $n = 6$ complex in fact could not find a minimum for the quintet species but did find a stable one for the triplet. The structure has C_{2h} symmetry, but as shown in Figure 5 this is quite close to an octahedral structure. The predicted vibrational bands lie at $2225/2227 \text{ cm}^{-1}$, which blend to make one band at our resolution. As Figure 10 shows, the agreement between this predicted spectrum and the measured one is quite good, suggesting that the $n = 6$ complex does indeed

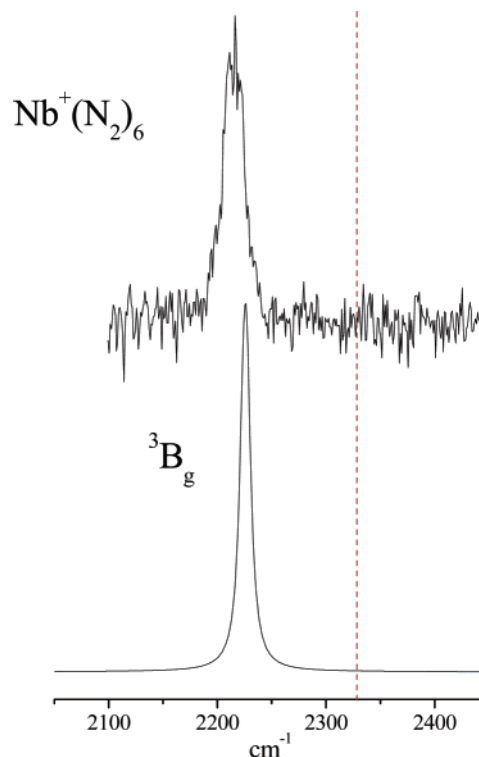


Figure 10. Comparison of the vibrational spectrum measured for $\text{Nb}^+(\text{N}_2)_6$ to the prediction of theory for the complex in the triplet spin state.

have a structure close to octahedral and that the electronic state is also a triplet. The ESR spectrum of neutral $\text{Nb}(\text{N}_2)_6$ provided evidence for a reduced symmetry D_{4h} complex caused by Jahn–Teller distortion.²³ It is interesting to note that niobium forms octahedral or near-octahedral structures in the condensed phase as well.⁹

The spectrum of $\text{Nb}^+(\text{N}_2)_7$ is basically the same as the $n = 6$ complex except that it has a much better signal-to-noise level. As discussed above, several pieces of evidence indicate that Nb^+ has a coordination of six N_2 ligands, and the $n = 7$ complex and larger ones studied here presumably have external ligands bound by van der Waals forces, with perhaps some binding enhancement caused by metal-induced polarization of the inner-sphere ligands. The more efficient dissociation for these larger complexes is then understandable. It is not possible to make detailed conclusions about the structures of these larger clusters, and indeed the van der Waals binding would probably lead to various orientations of the external ligands that would have similar binding energies. However, because there is a single vibrational resonance (Figure 3) and because this occurs at essentially the same position as those for the $n = 5$ and 6 complexes (near 2212 cm^{-1}), we can presume that larger complexes represent an $n = 6$ species with its complete ligand coordination sphere that is progressively solvated by excess nitrogen molecules. As discussed above, the red-shifted resonance at this position is associated with N_2 ligands perturbed by the metal ion binding, whereas the outer ligands have essentially no IR activity and are not contributing any strong bands to these spectra. The growing clusters apparently preserve the basic symmetry of the core $n = 6$ unit, because the spectrum does not shift substantially nor does it break up into any multiplet band structure. However, as shown in Table 2, the position of the one peak in the spectra of the larger clusters is

(52) Maitre, P.; Bauschlicher, C. W., Jr. *J. Phys. Chem.* **1995**, *99*, 6836.

(53) Bushnell, J. E.; Kemper, P. R.; Bowers, M. T. *J. Phys. Chem.* **1993**, *97*, 11628.

not always at exactly the same position. It shifts to slightly lower frequency values as cluster size increases. This is presumably the effect of the core unit being progressively more confined in the interior of the growing cluster. Likewise, the absence of any abrupt change in this band position also suggests that the $n = 6$ complex and all the larger ones are also triplets. Ligand crowding is one of the main considerations in the progressive shift to low-spin structures, and this effect remains in effect for the larger complexes.

Although the present data and theory present a consistent picture of the electronic structure and bonding in this system, some concerns with this study remain. Because of the problems that DFT has with the relative energies of different spin configurations, the agreement between the predicted and measured cluster size where the spin change occurs may be completely fortuitous. However, while quantitative energetics of different electronic states may be suspect, the vibrational spectrum predicted by DFT for a given electronic state should be reliable. As shown, the differences predicted for the vibrational spectra in quintet versus triplet states are significant. Because the agreement between these predicted spectra and those observed is quite acceptable, it is clear that the spin configuration change does indeed occur at the cluster size of $n = 5$ and beyond.

Another source of some concern is the large number of isomeric structures that may be produced for these clusters beyond those investigated with the present calculations. We examined all isomers for the $n = 2$ complex and a selected number for the $n = 3$ complex, and then assumed that the trends (i.e., unfavorable bonding for T complexes) could be extrapolated to larger clusters. However, we did show that T configurations and triplet electronic states lead to strong vibrational redshifts. Because our spectroscopic coverage does not extend below about 2100 cm^{-1} , it is conceivable that we might have missed some isomers of these types whose spectra appear at lower frequencies. On the other hand, any mixed isomers having both L and T configurations would have also had L-type N_2 vibrations in the spectral region covered here and would have produced additional bands beyond the single-peak spectra that we observed. The only clusters that we could have missed would be those with *all-T* configurations. If T configurations are actually stable (in contradiction to our DFT results on the small clusters), it is not clear why mixed configuration clusters would not also be found. Likewise, if intracluster reactions occurred to form nitrides or perhaps nitrogen metallocycle structures, some vibrations would occur below 2000 cm^{-1} where we would miss them. Again, however, *all* the N_2 molecules would have to be in such a configuration or else we would see some higher frequency bands. Because we see such simple spectra that all occur in the L- N_2 region, it is safe to assume that T configurations (or intracluster reactions) actually are unfavorable as predicted and that we have accounted for the major isomeric structures of these clusters. To test this conclusion, and to provide additional tests of other vibrational modes for all these clusters, future studies with improved IR lasers should probe the lower frequency region for these systems.

As a final point, it is interesting to compare the spectra seen previously for the $\text{V}^+(\text{N}_2)_n$ ³⁶ complexes to those seen here for $\text{Nb}^+(\text{N}_2)_n$. In both families of metal-nitrogen complexes, the N-N stretches are found to produce resonances with good IR

intensities, and these are red-shifted from the resonance of the free N_2 molecule. However, for each corresponding cluster size, the shifts for the $\text{Nb}^+(\text{N}_2)_n$ complexes are greater than those for the $\text{V}^+(\text{N}_2)_n$ by about $60\text{--}80\text{ cm}^{-1}$. Because ligands such as N_2 and CO are π -acceptors, all theoretical studies agree that π -back-donation from the TM is more important than ligand σ -donation in the TM- N_2 bond.^{10,12} The 4d-5s orbitals of the second-row TMs are more diffuse than the 3d-4s orbitals of the first-row systems, and hence metals such as Nb can back-donate electron density more effectively than their first-row counterparts.¹² As a result, Nb^+ can perturb the N_2 ligand to a larger degree than V^+ . This qualitative prediction of the DCD model agrees well with the spectral trends for these two $\text{TM}^+(\text{N}_2)_n$ systems that have been studied thus far. Additional studies on other $\text{TM}^+(\text{N}_2)_n$ complexes would be interesting to probe the details of electronic structure for different metals.

Conclusion

Nb^+ complexes from three up to 16 nitrogen molecules have been produced by laser vaporization and studied with infrared laser photodissociation spectroscopy. Small clusters ($n = 1\text{--}3$) are difficult to dissociate with infrared radiation, consistent with their expected strong metal-ligand bonding. Clusters with more than three ligands dissociate readily with IR excitation, and the larger complexes eliminate multiple nitrogen molecules. The fragmentation patterns of these larger complexes terminate at the $\text{Nb}^+(\text{N}_2)_6$ complex, indicating that niobium cation has a preferred coordination of six in these complexes. A secondary coordination of $n = 4$ is suggested by the mass spectral intensities, but this is not confirmed by other measurements. The infrared photodissociation in these complexes has strong resonances in the region of the N-N stretch; nitrogen ligands apparently obtain IR activity via their strong interaction with the metal cation. The N-N stretch resonances in all of these complexes are red-shifted with respect to the N-N stretch in the free nitrogen molecule. This reduced N-N frequency is consistent with the DCD model of metal complexation and has the same mechanism that explains red-shifted C-O stretches in metal-carbonyl complexes. DFT calculations are employed to probe both the geometric and electronic structures of these complexes. In the $n = 1, 2, 3$ complexes, theory suggests that the lowest-energy structures have N_2 ligands binding in end-on configurations with the Nb^+ in its quintet spin state. However, spectra cannot be obtained with sufficient signal levels to confirm these predictions. The $n = 4$ complex is predicted to have similar end-on ligand configurations, with the four ligands in a square-planar geometry, and the same quintet metal state. Its IR spectrum is found to be completely consistent with these predictions. DFT also predicts end-on binding for the $n = 5$ complex, with the ligands arranged in a geometry that is nearly a square pyramid. However, the progressive effects of multiple ligand binding are predicted to switch the metal spin in this system to a low-spin triplet state. Consistent with this, the $n = 5$ complex has a single main band that is shifted much further to the red than the $n = 4$ spectrum. The $n = 6$ complex has a single band, indicating a high-symmetry structure, and this is suggested to be near-octahedral, also with end-on ligand binding. The band position for the $n = 6$ and all higher complexes lies at essentially the same position as that for the $n = 5$ complex.

By comparison with theory, the resonance at this position is also consistent with a triplet spin state for the $n = 6$ complexes. Larger complexes apparently represent the $n = 6$ core ion enclosed in a growing shell of van der Waals-bound N_2 molecules.

Infrared spectroscopy of these gas-phase complexes provides appealing examples of coordination and ligand field interactions in the absence of perturbations from solvent or solid lattices. Direct comparisons to the predictions of theory can be made, with the caveat that theory still has difficulties with these transition-metal systems. As theoretical and experimental meth-

ods improve, cluster studies such as these will provide additional insights into metal–molecular interactions.

Acknowledgment. We are grateful for support from the U.S. Department of Energy through Grant No. DE-FG02-96ER14658.

Supporting Information Available: Full list of authors for ref 43 and a complete account of DFT calculations for all complex sizes and studied isomers. This material is available free of charge via the Internet at <http://pubs.acs.org>.

JA0661008